Energies **2012**, *5*, 3534-3549; doi:10.3390/en5093534

OPEN ACCESS

energies

ISSN 1996-1073

www.mdpi.com/journal/energies

Article

A Method for Balancing a Single-Phase Loaded Three-Phase Induction Generator

Yaw-Juen Wang and Ming-Hsueh Lee *

Graduate School of Engineering Science and Technology, National Yunlin University of Science & Technology, 123 University Road, Section 3, Douliou, Yunlin 64002, Taiwan;
E-Mail: wangyj@yuntech.edu.tw

* Author to whom correspondence should be addressed; E-Mail: g9310807@yuntech.edu.tw; Tel.: +886-5534-2601; Fax: +886-5531-2065.

Received: 18 May 2012; in revised form: 23 August 2012 / Accepted: 10 September 2012 / Published: 13 September 2012

Abstract: When a three-phase induction generator (IG) supplies unbalanced loads, its terminal voltages and line currents are also unbalanced, which may cause the IG to overheat and need to be derated. A single-phase loaded self-excited induction generator (SEIG) works under most unfavorable load unbalance conditions. This paper proposes a three-capacitor circuit scheme and a method to find the values of the self-excitation capacitors that allow the SEIG to be balanced. The SEIG is modeled by a two-port network equivalent circuit that resolves the SEIG into its positive- and negative-sequence circuits associated with the self-excitation capacitors and the load. The network can then be analyzed by common AC circuit analysis techniques. Successful results for balancing the SEIG supplying a single-phase load have been achieved by properly choosing the values of the excitation capacitors. The proposed method has also been validated by experiments on a 0.37 kW SEIG.

Keywords: induction generator; unbalance; single-phase load

Symbols and Acronyms

C_1, C_2, C_3	excitation capacitances
F	per-unit frequency
I_0, I_p, I_n	zero-, positive- and negative-sequence currents
I_a, I_b, I_c	three-phase line currents
I_m	magnetizing current
I_r	positive-sequence component of the rotor current

I_{sp}, I_{sn}	positive- and negative-sequence stator currents
R_s, R_r	stator and rotor resistances
v	per-unit speed
V_a, V_b, V_c	three-phase phase voltages
V_g	air-gap voltage
V_p, V_n	positive- and negative-sequence voltages
X_{cr}	critical magnetizing reactance
X_m	magnetizing reactance
X_{mn}	negative-sequence magnetizing reactance
X_s, X_r	stator and rotor reactances
y_1, y_2, y_3	load admittances
y_α, y_β, y_d	functions of y_1, y_2 and y_3 defined by Equation (6)
Y_L	admittance looking to the right of terminals *h* and *k* in Figure 3
Y_{nth}	admittance to the right of terminals *l* and *m* in Figure 3
Y_r	rotor admittance
Y_s	stator admittance
Y_T	function of Y_r, Y_s and Y_L defined by Equation (15)
Z_L	single-phase load impedance
$\boldsymbol{V}$, $\boldsymbol{I}$	voltage and current vectors
$\boldsymbol{V}_s$, $\boldsymbol{I}_s$	voltage and current symmetrical component vectors
$\boldsymbol{Y}$	nodal admittance matrix
$\boldsymbol{Y}_s$	similarity transformation of admittance matrix $\boldsymbol{Y}$
α	firing angle
τ	voltage unbalance factor
CUF	current unbalance factor
IG	induction generator
IM	induction motor
SEIG	self-excited induction generator
SVC	static var compensator
TCR	thyristor-controlled reactor
VUF	voltage unbalance factor

1. Introduction

Induction generators (IGs) are receiving more attention than in the past because of their low prices, simple construction, little maintenance, ruggedness and the fact they do not need dc sources and brushes, which make them particularly suitable as an energy conversion device for renewable energy sources such as wind, biogas and micro-hydro. In many developing countries where a significant percentage of the population and areas still suffer from electricity shortages, employing IGs for

generating electricity from renewable energy has become an important means of rural electrification and reduction of greenhouse gases emissions [1].

IGs can be operated in stand-alone or grid-interactive mode. In grid-interactive mode, an IG is directly connected to the grid that imposes its voltage and frequency and supplies the required reactive power. The analysis of a grid-connected IG does not differ much from that of an induction motor (IM). On the other hand, in stand-alone mode, self-excitation capacitors are needed to supply reactive power to the generator and load, and the generated voltage and frequency depend on the rotational speed, the load impedance and the values of excitation capacitors. Hence, the analysis of a self-excited induction generator (SEIG) is more complicated.

People living off the grid in remote islands, rural or mountain areas usually have single-phase type loads. Hence, a single-phase SEIG is an ideal option for electric power supply. While high capacity single-phase IMs up to 10 hp are available in the market, three-phase IMs above 5 hp (3.7 kW) are cheaper than single-phase IMs of the same ratings [2]. The use of a three-phase IM operated as an SEIG to generate single-phase electricity has been employed in many places for economic reasons. However, a three-phase SEIG operated as a single-phase generator is working under a very unbalanced condition, necessitating it to be derated to avoid overheating.

In the literature, studies on the three-phase SEIG feeding single-phase loads can roughly be categorized into two groups. The first group endeavors to minimize the voltage regulation and at the same time maximize the single-phase power output of the generator by properly choosing the values of the self-excitation capacitors, considering possible changes in the rotational speed of the prime mover. To mention some examples, Wang and Cheng [3] determined the minimum and maximum values of a single excitation capacitor required by a three-phase SEIG supplying a single-phase resistive load using the eigenvalue sensitivity method. Fukami *et al*. [4] proposed and analyzed a self-regulated three-phase SEIG working as a single-phase generator that consisted of two equal capacitors connected in series and another capacitor in parallel with the load resistor, and provided improved performance of voltage regulation. This generator scheme was further optimized by Mahato *et al*. [5] using the sequential unconstrained minimization technique to obtain a maximum power output for both capacitive and inductive single-phase loads.

The second group stresses the need for mitigating the voltage and current unbalance of a three-phase SEIG working as a single-phase generator. Al-Bahrani and Malik [6] analyzed the performance of a three-phase SEIG composed of a single capacitor in parallel with a single-phase load, *i.e.*, the single-phasing mode. Chan [7] developed a method based on symmetrical components for analyzing a three-phase SEIG supplying a single-phase load. Chan's method was applicable to the single-phasing mode as well as the Steinmetz connection. Chan and Lai [8,9] also developed a method to determine the minimum capacitance for voltage building-up of a three-phase SEIG with Steinmetz connection. It is noted that [6–9] only give methods for analyzing a three-phase SEIG feeding a single-phase load and do not report any method for balancing it. Chan and Lai [10] proposed a circuit scheme to balance the SEIG. In addition to the load resistance and excitation capacitance in the Steinmetz connection, they added an auxiliary load resistance and an auxiliary excitation capacitance. They used a phasor diagram to explain how to find the appropriate values of the auxiliary resistance and capacitance that allow a perfectly balanced three-phase voltage and current to be obtained. Alolah and Alkanhal [11] proposed another scheme that consisted of two excitation capacitors, the values of

which were determined using a sequential genetic and gradient optimization method. The voltage unbalance factor of the SEIG using the capacitance values found by that proposed algorithm was reported to range from 2% to 7%, showing a system that is not perfectly balanced.

In fact, achieving balanced loading on a three-phase generator provides benefits to the generator's performance which include: (1) making full use of the generator rating; (2) eliminating the pulsating torque caused by the negative-sequence current and hence reducing shaft mechanical vibration; and (3) eliminating voltage unbalance at the generator terminals caused by unbalanced load currents, which also improves voltage regulation of the generator.

In this paper, the authors propose a three-capacitor scheme that is able to perfectly balance a three-phase SEIG supplying a single-phase load. The three capacitors include a fixed capacitor that supplies the required reactive power to the system, and two variable capacitors that play the role of balancer. The two variable capacitors can be realized by two static var compensators (SVCs), a parallel combination of a fixed capacitor and a thyristor-controlled reactor (TCR). The three-capacitor scheme is represented by a two-port network IG model developed by Wang and Huang [12] for analysis. A solution method based on this two-port network model is also proposed for determining the values of the three capacitors. The circuit scheme and the method for finding capacitances to balance the SEIG are validated by comparing results obtained by the two-port network SEIG model and by experiments on a 0.375 kW induction generator.

2. Generator and Load Modeling

The two-port network model for a three-phase SEIG supplying unbalanced load developed in [12] is briefly described here and is used to analyze the proposed generator scheme. In addition, the voltage unbalance factor expressed as a function of the two-port network model's parameters is also derived.

2.1. Generator Scheme

Figure 1 shows the proposed three-capacitor scheme, which is composed of a Δ-connected three-phase induction machine and three capacitors C_1, C_2 and C_3 across each terminal pair. The single-phase load impedance Z_L is connected across terminals *a* and *b*. Capacitors C_2 and C_3 are variable according to the generator rotational speed and the load impedance, while C_1 is fixed and serves to supply additional reactive power to the machine and load. We note that the scheme shown in Figure 1 is indeed an IG supplying a Δ-connected unbalanced load composed of three admittances y_1, y_2 and y_3.

Figure 1. Three-capacitor scheme of SEIG feeding a single-phase load.

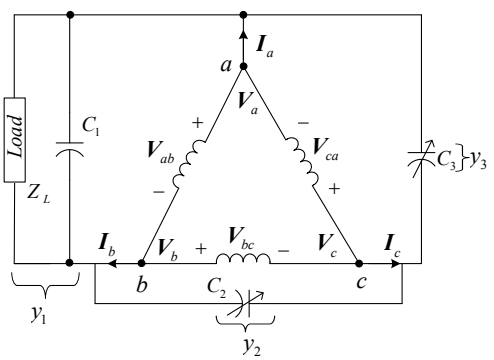

2.2. Modelling of an Unbalanced Three-Phase Load

Unbalanced loads can be combined and modeled as a Δ-connected three-phase load as shown in Figure 2a, where y_1, y_2 and y_3 are load admittances. Mixture of Y-connected and single-phase loads can also be converted to this model by appropriate transformation formulae. In Figure 2a, V_a, V_b and V_c refer to the phase voltages at the load terminals, and I_a, I_b and I_c to the line currents flowing into the load.

The relation between the three-phase voltages and currents can be written as:

$$\boldsymbol{I} = \begin{bmatrix} I_a \\ I_b \\ I_c \end{bmatrix} = \begin{bmatrix} y_3 + y_1 & -y_1 & -y_3 \\ -y_1 & y_1 + y_2 & -y_2 \\ -y_3 & -y_2 & y_2 + y_3 \end{bmatrix} \begin{bmatrix} V_a \\ V_b \\ V_c \end{bmatrix} = \boldsymbol{YV} \tag{1}$$

where $\boldsymbol{I}$ and $\boldsymbol{V}$ are current and voltage vectors, respectively; and $\boldsymbol{Y}$ the nodal admittance matrix. Let the corresponding symmetrical voltage and current component vectors be $\boldsymbol{V}_s$ and $\boldsymbol{I}_s$, respectively. $\boldsymbol{V}_s$ and $\boldsymbol{I}_s$ can be expressed as:

$$\boldsymbol{V}_s = \begin{bmatrix} V_0 & V_p & V_n \end{bmatrix}^T, \ \boldsymbol{I}_s = \begin{bmatrix} I_0 & I_p & I_n \end{bmatrix}^T \tag{2}$$

The subscripts 0, p and n refer to zero-, positive- and negative-sequence components, respectively. From Equation (1) and the symmetrical component equation for currents, we can write:

$$\boldsymbol{I}_s = \boldsymbol{A}^{-1}\boldsymbol{I} = \boldsymbol{A}^{-1}\boldsymbol{YV} = \boldsymbol{A}^{-1}\boldsymbol{YA}\boldsymbol{V}_s = \boldsymbol{Y}_s\boldsymbol{V}_s \tag{3}$$

where:

$$\boldsymbol{Y}_s = \boldsymbol{A}^{-1}\boldsymbol{YA}, \ \boldsymbol{A} = \begin{bmatrix} 1 & 1 & 1 \\ 1 & a^2 & a \\ 1 & a & a^2 \end{bmatrix}, \ a = 1\angle 120° \tag{4}$$

In Equation (4), $\boldsymbol{Y}_s$ is the similarity transformation of admittance matrix $\boldsymbol{Y}$. Equation (4) in a more detailed form can be given by:

$$\boldsymbol{Y}_s = \begin{bmatrix} 0 & 0 & 0 \\ 0 & y_d & y_\alpha \\ 0 & y_\beta & y_d \end{bmatrix} \tag{5}$$

where:

$$y_\alpha = -\left(ay_1 + y_2 + a^2 y_3\right), \ y_\beta = -\left(a^2 y_1 + y_2 + ay_3\right), \ y_d = y_1 + y_2 + y_3 \tag{6}$$

Hence, Equation (3) can be rewritten as:

$$\begin{bmatrix} I_0 \\ I_p \\ I_n \end{bmatrix} = \begin{bmatrix} 0 & 0 & 0 \\ 0 & y_d & y_\alpha \\ 0 & y_\beta & y_d \end{bmatrix} \begin{bmatrix} V_0 \\ V_p \\ V_n \end{bmatrix} \tag{7}$$

Since the zero-sequence current $I_0 = 0$, Equation (7) can be written in a more compact form as:

$$\begin{bmatrix} I_p \\ I_n \end{bmatrix} = \begin{bmatrix} y_d & y_\alpha \\ y_\beta & y_d \end{bmatrix} \begin{bmatrix} V_p \\ V_n \end{bmatrix} \tag{8}$$

Equation (8) implies a two-port network as shown in Figure 2b.

Figure 2. A delta-connected three-phase unbalanced load. (**a**) Circuit showing the nodal voltages and line currents; (**b**) The corresponding two-port network equivalent circuit.

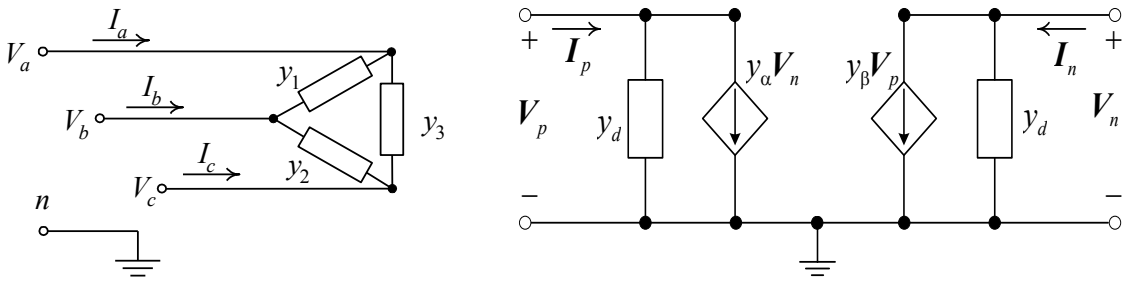

(**a**) (**b**)

2.3. Combination of Load and Generator Models

The load model shown in Figure 2b and the generator positive- and negative-sequence equivalent circuits can be combined to represent the SEIG with unbalanced loads. It is noted that voltages V_p and V_n and admittances y_α, y_β and y_d shown in Figure 2b need to be corrected by the per-unit frequency F. The complete sequence network of the SEIG with unbalanced loads is depicted in Figure 3, in which the left part is the positive-sequence network while the right part is the negative-sequence network. The two parts interact with each other through two dependent current sources. The effects of load unbalance are clearly expressed by parameters y_α, y_β and y_d. It is noted again that y_α, y_β and y_d are functions of F. When three-phase loads are balanced, *i.e.*, $y_1 = y_2 = y_3$, both y_α and y_β are equal to zero, implying no interaction between the positive- and the negative-sequence networks. The two-port equivalent circuit in Figure 3 fully represents the SEIG supplying unbalanced loads. A single-phase load is a particular case, and also the worst case, of unbalanced loads. In Figure 3, Y_r refers to the rotor admittance, Y_s to the stator admittance, and Y_L to the admittance looking to the right of terminals h and k. Y_{nth} is the admittance to the right of terminals l and m. Calculation of Y_{nth} is made easier if jX_{mn} is removed. This is a good approximation since the parallel branch $\left|(R_r/F+v)+jX_r\right|$ is much smaller than $\left|jX_{mn}\right|$, which gives:

$$Y_{nth} = y_d + \left[\frac{R_s}{F} + \frac{R_r}{F+v} + j\left(X_s + X_r\right)\right]^{-1} \tag{9}$$

The circuit shown in Figure 3 allows the positive-sequence stator current I_{sp} to be written as:

$$I_{sp} = Y_L \cdot \left(\frac{V_p}{F}\right) = y_d \cdot \frac{V_p}{F} + y_\alpha \cdot \frac{V_n}{F} \tag{10}$$

in which V_n/F can be given by:

$$\frac{V_n}{F} = -\frac{1}{Y_{nth}} \cdot y_\beta \cdot \frac{V_p}{F} \tag{11}$$

Combining Equations (10,11) allows I_{sp} to be written as:

$$I_{sp} = \left(y_d - \frac{y_\alpha y_\beta}{Y_{nth}} \right) \cdot \frac{V_p}{F} = Y_L \cdot \frac{V_p}{F} \tag{12}$$

which implies:

$$Y_L = y_d - \frac{y_\alpha y_\beta}{Y_{nth}} \tag{13}$$

Figure 3. Two-port network model of a three-phase SEIG with unbalanced load.

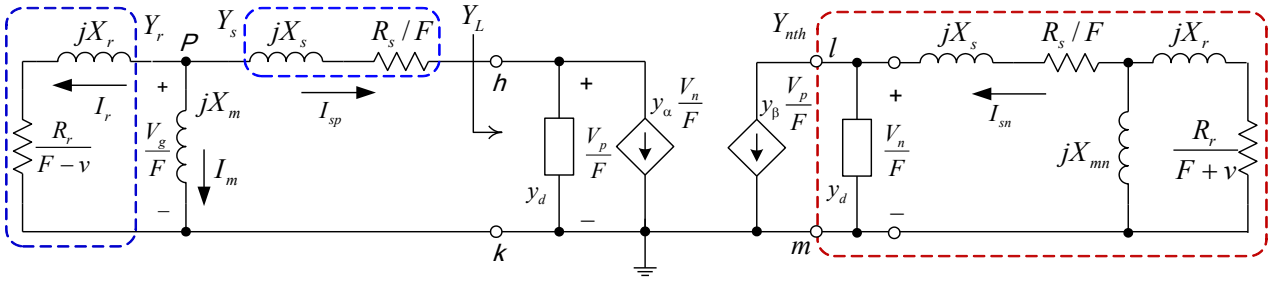

2.4. Analysis of the Sequence Networks

Analysis of the circuit of Figure 3 aims at finding the voltages and currents of the SEIG so that its performance under a specified operation condition can be predicted. In this paper, a two-step method is used to find the per-unit frequency F and the magnetizing reactance X_m in sequence. In Figure 3, we specify the air-gap voltage $\boldsymbol{V}_g$ to be the reference phasor. That is, $\boldsymbol{V}_g = V_g \angle 0°$. The magnetizing current I_m must be a pure imaginary quantity since the magnetizing reactance jX_m, which is a saturable reactance, is a pure imaginary quantity. The sum of the currents leaving node P equals zero, which means that $(I_r + I_{sp}) = -I_m$ is also an imaginary number. The sum $(I_r + I_{sp})$ can be given by:

$$I_r + I_{sp} = \frac{V_g}{F} Y_r + \frac{(V_g / F)}{Y_L^{-1} + Y_s^{-1}} = \frac{V_g}{F} \cdot \left(Y_r + \frac{Y_L Y_s}{Y_L + Y_s} \right) \tag{14}$$

Since V_g is a real quantity and $(I_r + I_{sp})$ an imaginary quantity, the real part of the admittance $Y_r + \dfrac{Y_L Y_s}{Y_L + Y_s}$ must be zero. If we define:

$$Y_T(F) = Y_r + Y_L Y_s / (Y_L + Y_s) \tag{15}$$

then the following relation holds:

$$Re[Y_T(F)] = Re[Y_r + Y_L Y_s / (Y_L + Y_s)] = 0 \tag{16}$$

Since Y_T is a function of Y_r, Y_s and Y_L, it is also a function of the per-unit frequency F. Equation (16) has only one unknown F, and can be solved for F using a numerical method such as the secant method or the false position method [13]. Determination of F does not need to know the value of X_m, largely simplifying the analysis. Once F is obtained by solving Equation (16), Y_T can then be found. Note that Y_T is indeed the total admittance in parallel with jX_m. The following relation holds:

$$I_m(jX_m + 1/Y_T) = 0 \tag{17}$$

Hence, we have:

$$jX_m = -1/Y_T \tag{18}$$

After the per-unit frequency F is obtained, the air-gap voltage V_g is to be determined. Figure 4 shows that the working point is at the intersection of the magnetizing curve and a load line defined by the equation:

$$V_g/F = jX_m \cdot I_m = -I_m/Y_T \tag{19}$$

Figure 4. Determination of the air-gap voltage V_g and the maximum magnetizing reactance X_{cr}.

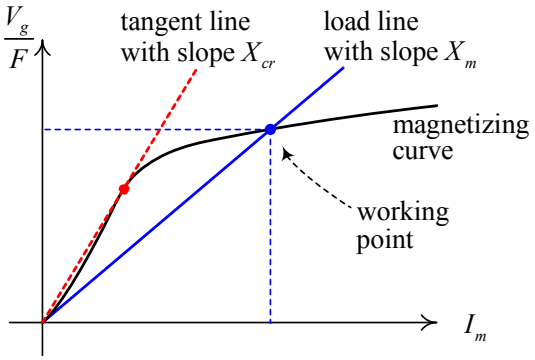

The expression of Y_T has been given in Equation (15). An iterative procedure can be taken to find the working point. The iterative procedure starts at an initial value of V_g or I_m, and finally converges at the intersection point. It is noted that the magnetizing curve must be obtained from the experiment. As shown in Equation (19), the slope of the load line is equal to X_m, which is a function of the rotational speed, the load impedance Z_L and the excitation capacitances C_1, C_2 and C_3. When the load line is just tangent to the magnetizing curve as shown by the (red) tangent line in Figure 4, X_m attains a critical value X_{cr} over which the generator is unable to build voltage. Hence, comparing the obtained X_m with X_{cr} is a useful criterion to judge if the generator can build voltage.

When F, V_g and I_m are known, all the voltages and currents in Figure 3 are easily obtainable. The voltages and currents shown in Figure 3 are positive- and negative-sequence components that need to be converted into the phase domain to find the corresponding three-phase quantities. An important quantity is the voltage unbalance factor τ, defined as the magnitude of the ratio of the negative- to positive-sequence voltage. From (11), the voltage unbalance factor τ can be expressed as a function of y_β and Y_{nth}:

$$\tau = VUF = \left|\frac{V_n}{V_p}\right| = \left|\frac{y_\beta}{Y_{nth}}\right| \tag{20}$$

3. The Solution Method

The analysis in Section 2 reveals that the voltage unbalance factor τ of the SEIG is determined by the ratio of y_β to Y_{nth}. When the SEIG is working at a balanced condition, the voltage unbalance factor τ must be equal to zero, which means that the numerator of Equation (20) is zero. Namely, the real and imaginary parts of admittance y_β must both be zero. These two conditions combined with the relation

for the per unit frequency F described by Equation (16) allow the following three simultaneous nonlinear equations to be written:

$$Re\left[y_{\beta}(F)\right] = Re\left[-(a^2 \cdot y_1 + y_2 + a \cdot y_3)\right] = 0 \tag{21}$$

$$Im\left[y_{\beta}(F)\right] = Im\left[-(a^2 \cdot y_1 + y_2 + a \cdot y_3)\right] = 0 \tag{22}$$

Given that C_1 and Z_L are known, the values of F, C_2 and C_3 can be found by solving Equations (16,21,22) using the Newton-Raphson method if appropriate initial guess values are provided. The obtained values of C_2 and C_3 allow the SEIG to work at a balanced condition. In comparison with the Hooke and Jeeves search technique used in Chan's work [7], the proposed method of directly solving three simultaneous nonlinear equations is much easier. In this paper, the nonlinear simultaneous equations have been solved using Mathcad [13], which is a widely used general-purpose mathematic software tool.

4. Numerical Applications

An induction motor working as an SEIG supplying a single-phase load has been used to illustrate the proposed methods for solving C_2 and C_3 to balance the generator. It has been set up as shown in Figure 5. The generator is a 3-phase, 220-V, Δ-connected, 60-Hz, 4-pole, 1/2 hp squirrel-cage induction machine. The motor characteristics and test methods for obtaining the parameters of the generator equivalent circuit are given in the appendix. Also included in the appendix are the test method for the magnetizing saturation curve, and how the fixed capacitor C_1 is determined in this study.

Figure 5. Experimental set-up of an SEIG feeding a single-phase load.

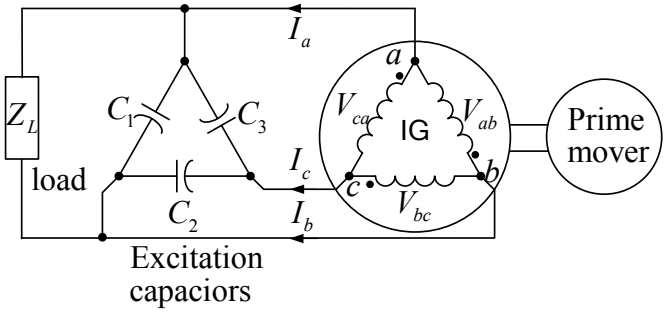

In the following sections, we firstly show a few examples of applying the proposed solution method for finding the values of C_2 and C_3 that balance the generator when Z_L, C_1 and the rotational speed are known. The example that follows is the use of the capacitance values found by the solution method for the experiment on the 1/2 hp squirrel-cage induction machine to see whether the generator is working under balanced conditions.

4.1. Verification of the Obtained Capacitance Values

The solution method described in Section 3 has been employed to find the values of C_2 and C_3 when the generator runs at 1764 rpm and C_1 is fixed to 10 μF. The solved results for resistive loads

Z_L = 400 Ω and Z_L = 1000 Ω, and inductive loads Z_L = 500 + *j*1130.97 Ω and Z_L = 467.13 + *j*123.91 Ω (at 60 Hz) are shown in Table 1.

In the table, the values of τ corresponding to the solution values of C_2 and C_3 are also listed, being all very close to zero and showing that the obtained capacitance values can balance the generator. The values of the magnetizing reactance X_m listed in Table 1 are all smaller than X_{cr}/F, meaning that the capacitance values obtained allow the generator to build voltage.

Table 1. Capacitance values C_2 and C_3 and the resulting voltage unbalance factor for different load impedances at a rotating speed of n = 1764 rpm.

***n* (rpm)**	**1764**			
***Z*$_L$ (Ω)**	**400 Ω**	**1000 Ω**	**R-L (series) R = 500 Ω, L = 3000 mH**	**R//L (parallel) R = 500 Ω, L = 5000 mH**
C_2 (μF)	13.98	11.58	8.490	11.66
C_3 (μF)	6.019	8.421	7.420	5.321
τ (%)	1.86×10^{-6}	2.97×10^{-7}	1.62×10^{-7}	3.7×10^{-7}
P_{out} (*W*)	125.76	57.27	9.17	59.20
F (p.u.)	0.96182	0.97004	0.97543	0.96590
I_m (*A*)	1.36	1.49	0.83	0.90
X_m (Ω)	93.44	89.10	110.98	108.98

The values of C_2 and C_3 solved by the proposed method for operating conditions of n = 1800 rpm with load Z_L equal to 500, 2000, 600 + *j*1357.16 and 373.7 + *j*99.12 Ω (at 60 Hz), respectively, are listed in Table 2, in which the resulting voltage unbalance factors τ are small too, verifying that the obtained capacitance values can balance the generator. Checks on the magnetizing reactance X_m also assure building-up of the generator voltage.

Table 2. Values of C_2 and C_3 for different load impedances at a speed of n = 1800 rpm.

***n* (rpm)**	**1800**			
***Z*$_L$ (Ω)**	**500 Ω**	**2000 Ω**	**R-L (series) R = 600 Ω, L = 3600 mH**	**R//L (parallel) R = 400 Ω, L = 4000 mH**
C_2 (μF)	13.11	10.77	8.769	12.07
C_3 (μF)	6.887	9.229	7.930	4.285
τ (%)	3.18×10^{-7}	1.94×10^{-7}	0.0041	0.00019
P_{out} (*W*)	118.98	33.22	12.35	69.35
F (p.u.)	0.98395	0.99249	0.99528	0.98297
I_m (*A*)	1.53	1.66	1.14	0.85
X_m (Ω)	88.09	84.13	100.93	110.46

The values of C_2 and C_3 found for operating conditions of n = 1836 rpm with load Z_L equal to 600, 3000, 700 + *j*1507.96 and 560.55 + *j*148.69 Ω (at 60 Hz), respectively, are summarized in Table 3. The resulting voltage unbalance factors are again very close to zero. Voltage building-up is also checked for each loading condition.

Table 3. Values of C_2 and C_3 for different load impedances at a speed of n = 1836 rpm.

***n* (rpm)**	**1836**			
Z_L (Ω)	**600 Ω**	**3000 Ω**	**R-L (series) R = 700 Ω, L = 4000 mH**	**R//L (parallel) R = 600 Ω, L = 6000 mH**
C_2 (μF)	12.54	10.50	8.961	11.38
C_3 (μF)	7.461	9.496	8.215	6.306
τ (%)	1.12×10^{-6}	5.88×10^{-9}	2.25×10^{-7}	3.97×10^{-8}
P_{out} (*W*)	113.21	24.73	14.03	89.10
F (p.u.)	1.00527	1.01311	1.01499	1.00648
I_m (*A*)	1.67	1.79	1.35	1.31
X_m (Ω)	83.59	80.28	93.93	95.05

4.2. Experimental Results

The 1/2 hp squirrel-cage induction machine operating as an SEIG is set up as shown in Figure 5 for experiments. The SEIG's rotational speed and excitation capacitor C_1 are fixed at 1800 rpm and 10 μF, respectively. Both pure resistive loads and inductive loads are tested.

For the case of pure resistive loads, when the load Z_L varies from 500 to 2000 Ω, the proposed solution method is used to find the corresponding values of C_2 and C_3 that balance that generator. These capacitance values are then used in the two-port network model and in the experiments. The capacitance values obtained by the solution method are directly used as the inputs to the two-port network method. However, for the experiments, the (parallel and series combinations of) capacitors with values closest to the calculated values are used. Table 4 lists the load resistance values, the capacitance values calculated by solving Equations (16,21,22), the capacitance values actually used in the experiments, the measured values of voltage unbalance factor (VUF) and the current unbalance factor (CUF). The measured VUF values listed in Table 4 are all lower than 1%, validating the proposed method. Figure 6 compares the measured values (scattered dots) of frequency, three-phase voltages, currents and output power, with the results obtained by the proposed analytical method (solid lines), for the resistive load continuously varying from 500 to 2000 Ω. Good agreement has been achieved. The comparison of line voltages and currents depicted in Figures 6(b,c) only shows the values in one phase for the calculated results (solid lines) since the calculated voltages and currents are nearly perfectly balanced. Nevertheless, the measured three-phase voltages and currents are given in detail to allow the unbalance to be observed.

The experimental results for inductive loads are summarized in Table 5. Since the impedance value does not vary continuously, it is not appropriate to present these results graphically, so only a table is given. In this table, both calculated and actually used capacitance values are listed. The load resistance is easily adjusted using a rheostat, but the load inductance is more unstable because of magnetic saturation. The experiment has been carried out by firstly choosing an approximate value of inductance, and then finding its accurate inductance value by calculation from the measured voltage and current of the inductor. After the load resistance and inductance are obtained, the same procedure as in the case of pure resistive loads has been followed to find the capacitances C_2 and C_3. Also listed in Table 5 are measured VUF and CUF values. Except for the first row, the VUF values are all lower than 1%. The

VUF value in the first row is higher because the value of C_3 used in the experiment deviates slightly more significantly from its theoretical value than those in other rows.

Figure 6. Comparison of the results obtained by experiments (scattered dots) and by the analytical method (solid line) for resistive load Z_L varying from 500 Ω to 2000 Ω. (**a**) Frequency; (**b**) Line voltages; (**c**) Line currents; (**d**) Output power.

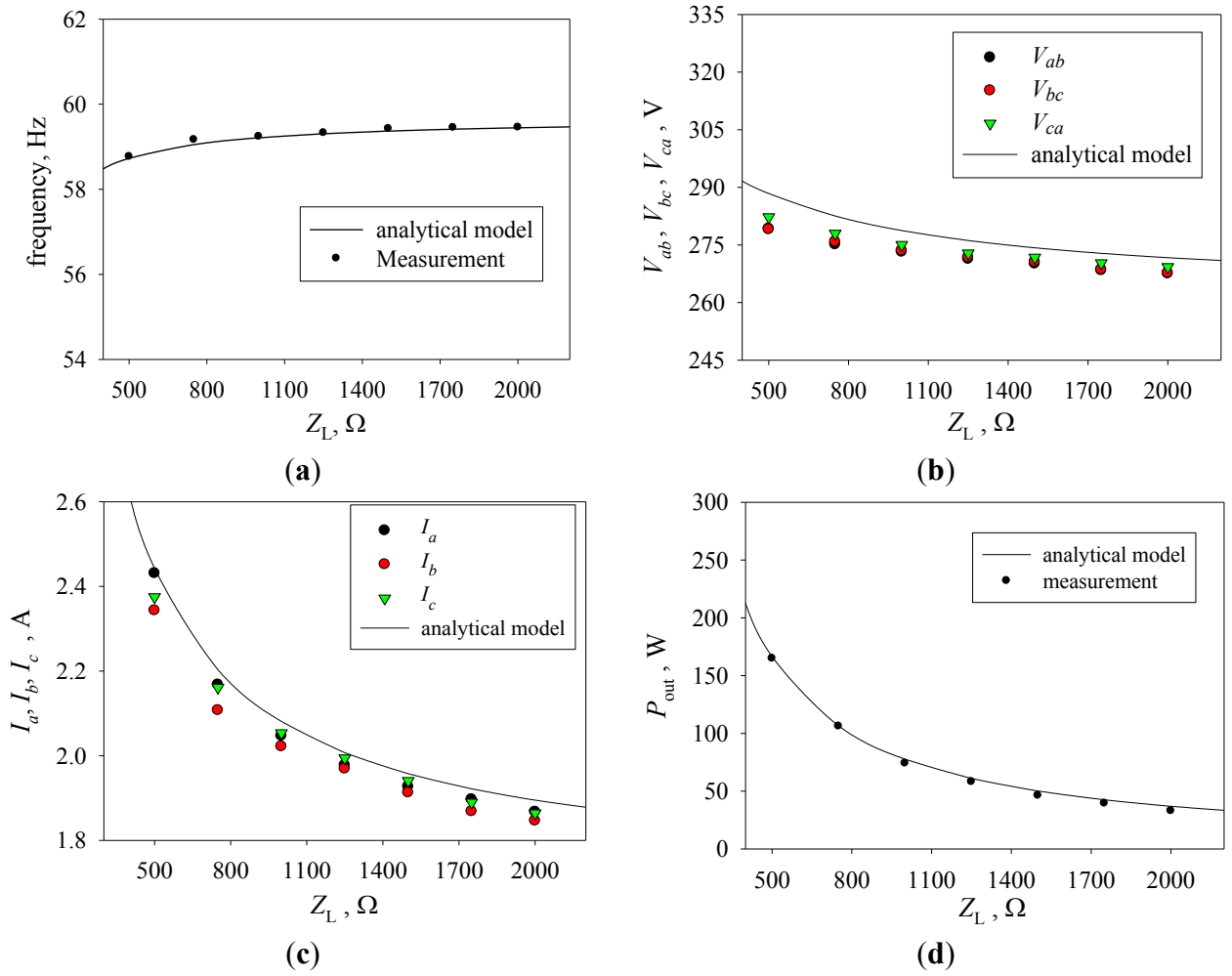

Table 4. Theoretical and experimental capacitance values and measured VUF and CUF for pure resistive loads.

Z_L (Ω) (resistive)	Theoretical		Experimental			
	C_2 (μF)	C_3 (μF)	C_2 (μF)	C_3 (μF)	VUF (%)	CUF (%)
500	13.11	6.888	13.2	6.8	0.74	1.96
750	12.07	7.933	12.1	8.0	0.60	1.70
1,000	11.55	8.452	11.5	8.5	0.40	0.82
1,250	11.24	8.763	11.2	8.7	0.31	0.62
1,500	11.03	8.970	11.0	9.0	0.35	0.71
1,750	10.88	9.118	10.8	9.1	0.44	0.86
2,000	10.77	9.228	10.6	9.2	0.40	0.83

Table 5. Theoretical and experimental capacitance values and measured VUF and CUF for inductive loads.

$Z_L = R + j\omega L$		Theoretical		Experimental			
R (Ω)	L (mH)	C_2 (μF)	C_3 (μF)	C_2 (μF)	C_3 (μF)	VUF (%)	CUF (%)
50	1663.56	14.47	10.40	14.45	10.24	1.02	5.54
150	1701.34	14.49	11.07	14.60	11.07	0.28	0.84
400	1787.83	13.95	12.02	14.10	11.95	0.51	0.59
600	1888.30	13.27	12.14	13.35	12.10	0.21	0.46

5. Conclusions

This paper has proposed a three-capacitor circuit scheme that is able to balance an SEIG supplying a single-phase load. The three-capacitor scheme consists of a fixed capacitor and two variable capacitors. The fixed capacitor is chosen to compensate the reactive power required by the generator and the load, while the two variable capacitors serve to balance the generator according to the load impedance and the rotational speed of the generator.

In order to find the values of the two variable capacitors, a two-port network model of the SEIG has been employed to analyze the generator with arbitrary unbalanced loads. With the aid of this circuit model, a method that involves solving a set of three nonlinear simultaneous equations has been proposed to find the values of the two capacitors that minimize the voltage unbalance of the generator. The proposed method has further been validated by experiments on a 1/2 hp three-phase squirrel-cage induction motor working as an induction generator feeding a single-phase load. Both resistive and inductive single-phase loads have been tested and satisfactory results have been obtained.

Acknowledgments

This research was financially supported by the National Science Council of Taiwan, ROC, under grant number NSC101-2221-E-224-074.

Appendix

A.1. Generator Characteristics, Test Methods and Saturation Curve

The generator used is a squirrel-cage induction motor working as an SEIG. The motor is 3-phase, 220-V, Δ-connected, 60-Hz, 4-pole, and rated at 1/2 hp. The no-load test, the blocked-rotor test and the DC test for stator resistance were carried out to obtain the parameters of the motor equivalent circuit. The procedures of these tests are described in detail in most textbooks of electrical machines such as [14]. The equivalent circuit parameters are $R_s = 20.63\ \Omega$, $R_r = 15.85\ \Omega$, $X_s = X_r = 21.062\ \Omega$.

Another test for tracing the magnetizing saturation curve was also performed at 60 Hz ($F = 1$). The motor shaft was coupled to a synchronous motor to keep its speed at 1800 rpm. The three-phase motor terminal voltage was varied from nearly zero to a value that slightly overcurrented the motor. The terminal voltage subtracted by the voltage drop of the stator impedance allows the air gap voltage V_g to be found. The curve of the air gap voltage V_g against the measured stator current, which is in this

condition equal to the magnetizing current I_m, is the magnetizing saturation curve as shown in Figure A1. Figure A1 shows the measured results (scattered dots) and a curve with the expression:

$$\frac{V_g}{F} = \frac{a}{1+(I_m/b)^{-c}} \tag{A1}$$

where parameters a = 183.3082 V, b = 0.8697 A and c = 1.5704 were found using a nonlinear regression tool. Figure A1 allows the value of the critical magnetizing reactance X_{cr} to be obtained by drawing a straight line passing through the origin and tangent to the magnetizing curve. The slope of this line yields a good estimate of X_{cr}. The value X_{cr} = 113 Ω at 60 Hz (*i.e.*, F = 1.0) is used in the analysis. It is noted that this value needs to be corrected by the per-unit frequency F for a frequency other than 60 Hz.

Figure A1. Magnetizing curve of the SEIG.

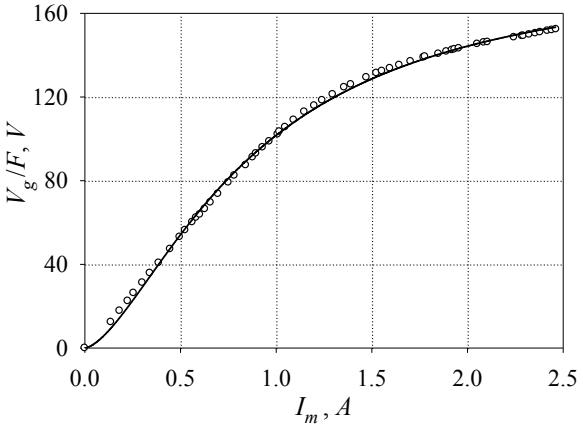

A.2. Determination of Capacitance C_1

Capacitance C_1 is set to a fixed value of 10 μF throughout the study. This value was obtained in the balanced loading test of the generator. When the excitation capacitors are all equal to 10 μF, *i.e.*, $C_1 = C_2 = C_3 = 10$ μF, and the three-phase load is also balanced, the generator easily builds up voltage over a wide range of load resistance. The value of 10 μF is thus taken as a fixed value for C_1 which is not variable in this study. In our tests, a higher value of C_1 also allows the generator to build up voltage easily, but the generator also attains an overcurrent condition. On the other hand, a lower value of C_1 sometimes fails to build up voltage. Hence, the value of 10 μF is a compromise of voltage building up and the generator current rating.

A.3. Physical Implementation of Variable Capacitors

The two variable capacitors C_2 and C_3 in Figure 1 serve to balance the generator. In electric grid applications, an old method of adjusting capacitance is the use of a no-load synchronous motor. Its excitation current is controlled to generate variable reactive power, and the synchronous motor acts as a variable capacitor. Modern power electronics technology has allowed this old method to be replaced by SVC which is composed of a TCR with a shunt capacitor, and has been extensively employed in the electric grid for reactive power control. The basic principle of SVC is illustrated in Figure A2. If a

variable capacitor across nodes *a* and *b* is needed as shown in Figure A2a, then a parallel combination of a fixed capacitor C_S and a variable inductor L (see Figure A2b) has the equivalent function as a variable capacitor. The variable inductor L can be realized by a TCR which is basically a fixed inductor L_T controlled by two back-to-back thyristors as shown in Figure A2c. By controlling firing angle α of the thyristors, the current flowing through inductor L_T can be adjusted continuously from a maximum value at full conduction to a minimum value (zero) at cut-off of the thyristors. Figure A3 shows a possible application of two SVCs for the implementation of variable capacitors C_2 and C_3 shown in Figure 1. By controlling firing angles α_1 and α_2, the capacitance values of C_3 and C_2 can be varied, respectively.

Figure A2. Basic principle of realizing a variable capacitor using an SVC. (**a**) A variable capacitor C; (**b**) A fixed capacitor C_S in parallel with a variable inductor L; (**c**) An SVC composed of a TCR with a shunt capacitor C_S.

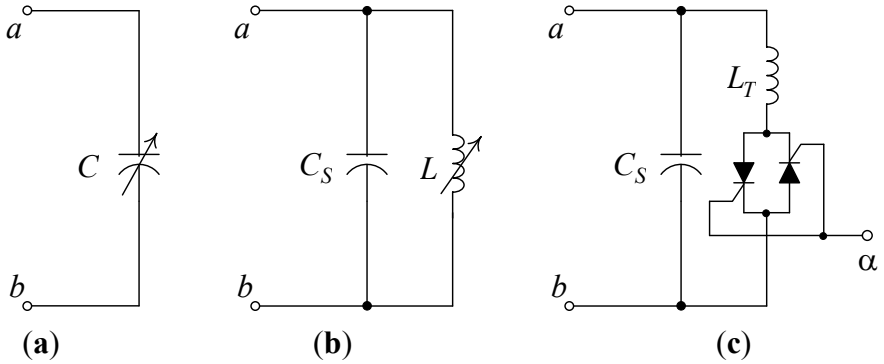

Figure A3. Implementation of variable capacitors C_2 and C_3 using two SVCs.

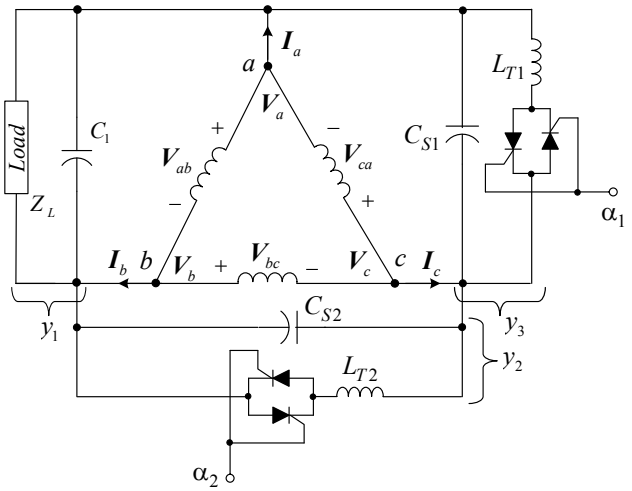

References

1. Murthy, S.S.; Singh, B.; Gupta S.; Gulati, B.M. General steady-state analysis of three-phase self-excited induction generator feeding three-phase unbalanced load/single-phase load for stand-alone applications. *IEE Proc. Gener. Transm. Distrib.* **2003**, *150*, 49–55.

2. Durham, M.O.; Ramakumar, R. Power system balancers for an induction generator. *IEEE Trans. Ind. Appl.* **1987**, *23*, 1067–1072.
3. Wang, L.; Cheng, C.M. Excitation capacitance required for an isolated three-phase induction generator under single-phasing mode of operation. In *Proceedings of International Conference of Power Engineering Society Winter Meeting*, Columbus, OH, USA, 27–31 January 2001.
4. Fukami, T.; Kaburaki, Y.; Kawahara, S.; Miyamoto, T. Performance analysis of a self-regulated self-excited single-phase induction generator using a three-phase machine. *IEEE Trans. Energy Convers*. **1999**, *14*, 622–627.
5. Mahto, S.N.; Singh, S.P.; Sharma, M.P. Capacitors required for maximum power of a self-excited single-phase induction generator using a three-phase machine. *IEEE Trans. Energy Convers*. **2008**, *23*, 372–381.
6. Al-Bahrani, A.H.; Malik, N.H. Steady-state analysis and performance characteristic of a 3-phase induction generator self-excited with a single capacitor. *IEEE Trans. Energy Convers*. **1990**, *5*, 725–732.
7. Chan, T.F. Performance analysis of a three-phase induction generator self-excited with a single capacitance. *IEEE Trans. Energy Convers*. **1999**, *14*, 894–900.
8. Chan, T.F.; Lai, L.L. Capacitance requirements of a three-phase induction generator self-excited with a single capacitance and supplying a single-phase load. *IEEE Trans. Energy Convers*. **2002**, *17*, 90–94.
9. Chan, T.F.; Lai, L.L. Comments to the paper "Capacitance requirements of a three-phase induction generator self-excited with a single capacitance and supplying a single-phase load". *IEEE Trans. Energy Convers*. **2004**, *19*, 222.
10. Chan, T.F.; Lai, L.L. Phase balancing for a self-excited induction generator. In *Proceedings of International Conference of Power Utility Deregulation, Restructuring and Power Technologies*, London, UK, 4–7 April 2000.
11. Alolah, A.I.; Alkanhal, M.A. Excitation requirements of three-phase self-excited induction generator under single-phase loading with minimum unbalance. In *Proceedings of International Conference of Power Engineering Society Winter Meeting*, Singapore, 23–27 January 2000.
12. Wang, Y.J.; Huang, S.Y. Analysis of a stand-alone three-phase self-excited induction generator with unbalanced load using a two-port network model. *IET Electr. Power Appl*. **2009**, *3*, 445–452.
13. Ansari, K.A. *An Introduction to Numerical Methods Using Mathcad*; Schroff Development Corp.: Spokane, WA, USA, 2007.
14. Chapman, S.J. *Electric Machinery Fundamentals*, 4th ed.; McGraw-Hill: Boston, MA, USA, 2005; pp. 452–460.